









# Microstructural characterization and quantitative analysis of the interfacial carbides in Al(Si)/diamond composites

Christian Edtmaier<sup>1,\*</sup> , Jakob Segl<sup>1</sup> , Erwin Rosenberg<sup>1</sup> , Gerhard Liedl<sup>2</sup> , Robert Pospichal<sup>2</sup> , and Andreas Steiger-Thirsfeld<sup>3</sup> 

<sup>1</sup>Institute of Chemical Technologies and Analytics, TU Wien, Getreidemarkt 9/164, 1060 Vienna, Austria

<sup>2</sup>Institute of Production Engineering and Laser Technology, TU Wien, Vienna, Austria

<sup>3</sup>USTEM - University Service Centre for Transmission Electron Microscopy, TU Wien, Vienna, Austria

Received: 27 April 2018

Accepted: 23 July 2018

Published online:  
30 July 2018

© The Author(s) 2018

## ABSTRACT

The existence of interfacial carbides is a well-known phenomenon in Al/diamond composites, although quantitative analyses are not described so far. The control of the formation of interfacial carbides while processing Al(Si)/diamond composites is of vital interest as a degradation of thermophysical properties appears upon excessive formation. Analytical quantification was performed by GC–MS measurements of gaseous species released upon dissolving the matrix and interfacial reaction products in aqueous NaOH solutions and the CH<sub>4</sub>/N<sub>2</sub> ratio of the evolving reaction gases can be used for quantification. Although the formation of interfacial carbides is significantly suppressed by adding Si to Al, also a decline in composite thermal conductivity is observed in particular with increasing contact time between the liquid metal and the diamond particles during gas pressure infiltration. Furthermore, surface termination of diamond particles positively affects composite thermal conductivity as oxygenated diamond surfaces will result in an increase in composite thermal conductivity compared to hydrogenated ones. In order to understand the mechanisms responsible for all impacts on the thermal conductivity and thermal conductance behaviour, the metal/diamond interface was electrochemical etched and characterized by SEM. Selected specimens were also cut by an ultrashort pulsed laser system to characterize interfacial layers at the virgin cross section in the reactive system Al/diamond.

Address correspondence to E-mail: christian.edtmaier@tuwien.ac.at

## Introduction

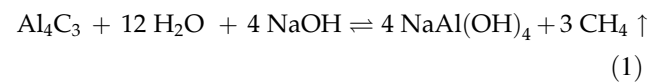
Monolithic materials cover a wide range of combinations of coefficient of thermal expansion (CTE) and thermal conductivity (TC); however, the required combination of highest thermal conductivity and lowest CTE is virtually not occupied. The most promising class of materials to reach thermal conductivity beyond that of copper or silver are metal matrix composites (MMCs) containing diamonds. Although these materials have received some interest since the early 1990s, most are still at scientific level, only very few companies commercialized such products.

Unfortunately, the diamond/metal contacts have a finite interface thermal conductance (ITC, or TBC, thermal boundary conductance). Even if perfect mechanical bonding is achieved at the interface, intrinsic interface thermal resistance (ITR) arises due to the scattering of phonons and electrons when travelling between materials with different elasticity and dielectric constants. The presence of limited heat flow across interfaces resulted in a high quantity of scientific investigations to improve bonding between matrix and inclusion phases and therefore heat transfer across the interface that may give access to an overall improved thermal conductivity of the composites.

Most of the work to improve ITC concerns the introduction of carbide-forming elements to form stronger chemical and physical bonds at the interface [1–6], which is especially of importance for matrix systems like copper and silver, which are both known not to wet and bond to carbon allotropes. In case of aluminium as matrix metal, the formation of carbides like  $\text{Al}_4\text{C}_3$  is well documented [7]. However, excessive formation of  $\text{Al}_4\text{C}_3$  is undesirable, as it has low thermal conductivity and readily corrodes in moist air to form aluminas, such as  $\text{Al}(\text{OH})_3$ . It is furthermore commonly accepted that  $\text{Al}_4\text{C}_3$  formation can be controlled by alloying Al with Si because of competitive formation of SiC and by the limitation of solubility of carbon in liquid aluminium which results in reduced capability to form  $\text{Al}_4\text{C}_3$  at given temperatures, respectively [6]. It is furthermore notable that a minimum concentration of  $\text{Al}_4\text{C}_3$  at the interface is essential to enhance thermal transport, as at very low concentration or even total absence of carbides, i.e. caused by rapid consolidation like

squeeze casting, a decrease in composite thermal conductivity is observed [6, 8].

In order to monitor the formation of  $\text{Al}_4\text{C}_3$  during infiltration, a method first employed by Simancik et al. [9] for the quantification of  $\text{Al}_4\text{C}_3$  by mass-spectrometric coupled gas chromatography technique (GC–MS) can be applied. This routine is based on the simple context, that  $\text{Al}_4\text{C}_3$  releases  $\text{CH}_4$  upon dissolving in aqueous media (Eq. 1). By measuring the  $\text{CH}_4$  amount in relation to the amount of  $\text{N}_2$ , used as an internal standard, the  $\text{Al}_4\text{C}_3$  content can be determined through prior calibration.



One less exploited aspect concerns the role of surface termination of diamond surfaces by oxygenation or hydrogenation on the Kapitza resistance and subsequently on the thermophysical properties of diamond MMCs [10–14]. From a scientific perspective, it is essential to understand how this interface has to be designed in order to minimize the Kapitza resistance and to improve ITC. So far, the role of surface termination of diamond surfaces on ITC was mainly shown on “clean-model” systems, i.e. well-defined plain and large synthetic diamond monocrystal surfaces with sputtered layers of Al and other metals creating a carbide-forming interlayer. The ITC is then calculated by means of TDTR time-domain thermoreflectance experimental setup [10, 11, 15]. In [14] the positive influence of oxygenation on ITC was for the first time shown to be true in the low (4 K) to ambient temperature range for a  $\text{Ag}_3\text{Si}$ /diamond system, fabricated under typical “messier” lab-scale conditions of gas pressure infiltration using synthetic diamond particles. Note, that different terminations of diamond surfaces can be created by acid and plasma treatments, respectively, and can result in the formation of different proportions of COOH, C–O, C=O, C  $sp^2$  and C  $sp^3$  bonding types depending on the applied chemicals and processes [10, 16, 17].

In the present work the influence of the contact time (i.e. the time between the liquid and the diamonds during the gas pressure infiltration process) on the thermal conductivity, the amount of  $\text{Al}_4\text{C}_3$  formed and the interfacial structure of the resulting MMCs are studied. Furthermore, the influence of the addition of Si as an alloying element on the aforementioned characteristics will be observed. As mentioned above, the aspect of surface termination of

diamond surfaces by oxygenation or hydrogenation is of interest for understanding thermal transport at the interface, thus, it is of interest to study its impact on  $\text{Al}_4\text{C}_3$  formation in dependence of process parameters like contact time and amount of Si in Al.

## Experimental procedure

Diamond/metal composites were produced by liquid metal infiltration of Al, Al0.5Si, Al1Si and Al3Si matrix materials into a tapped and vibrated powder bed of synthetic diamond grit of mesh sizes 70/80. The synthetic diamonds were of the SDB1125 type from E6 and purchased by *ServSix GmbH, Karlstein, Germany*. The Al–Si matrix alloys were inductively melted and cast using 3N8 Al and 4N Si base elements. The different Si concentrations in Al were properly selected due to the fact, that Al0.5Si represent an alloy of very low solubility of Si in the  $\alpha$ -Al, thus Si may be dissolved in the lattice or will form fine precipitates while cooling to ambient. Whereas in the Al1Si and Al3Si system, Si is formed—in different weight fractions—by the eutectic reaction during solidification.

Furthermore, the diamond particles were surface treated to create H- and O-termination, respectively. To create H-termination on the diamond surfaces, the as-received diamond powders were placed in a furnace at 1123 K in  $\text{H}_2$  gas atmosphere for 60 min. O-termination was realized by immersing diamonds in hot sulphuric acid for a period of 5 min, subsequently rinsed with de-ionized water and 2-propanol and finally dried at 383 K. Those treatments were accompanied by XPS measurements to confirm correct functionalization of diamond surfaces (results are given in [17]). Composites using such treated diamond particles are subsequently denoted as “H-terminated” and “O-terminated”, respectively.

The thermal conductivity samples were infiltrated net-shape. A solid piece of metal and metal alloy, respectively, was placed on top of the graphite preform filled up with diamond particles. Prior to melting, vacuum was applied in order to facilitate infiltration. After the infiltration temperature of roughly 1173 K had been reached, Argon gas pressure of 3 MPa was applied to force the liquid metal into the diamond powder bed. The heating was switched off after 1, 5 and 10 min (which is called the “contact time”  $t_c$  between the liquid and the

diamonds) and the infiltrated bodies were furnace cooled under pressurized condition within less than 20 min to room temperature. After cool down, composite pieces were dismantled from the die. This fast cooling process guarantees a rather precise determination of the contact time, however, it may also cause the system to be not in thermal equilibrium, for which reason composites were subsequently annealed at 573 K for 1 h in Argon atmosphere. The diamond volume fraction was determined by densitometry to be  $64 \pm 1$  vol.-pct for all MMCs. This is in good agreement with the relative densities of up to 99.5 pct., indicating that the composite samples were fully infiltrated and contained little, if any, porosity.

Thermal conductivity measurements were performed in a steady-state heat flow equipment close to ambient temperature. The thermal conductivity was determined by the temperature gradients in the serial arrangement of the sample and a reference. The gradient is established by a heating and a cooling circuit anchored between one side of the serial arrangement of the sample and the other side of the reference. Sample size is a rod of 8 mm diameter and an overall length of about 33 mm. The temperature evolution along the sample length  $L$  is controlled by means of Pt100 sensors. Experimental errors originating from the determination of the geometrical cross sections and active length of the given sample geometry may cause systematic errors. As a consequence, the composite thermal conductivity  $\kappa_c$  can become uncertain. Based on simultaneous measurements of the thermal and the electrical conductivity of the matrix alloy alone, and taking into account composite theory we conclude that the uncertainty on the thermal conductivities measured by the present method is < 3 pct.

As aluminium carbide  $\text{Al}_4\text{C}_3$  is formed by reaction between diamonds and aluminium [18, 19] it is of interest to quantify its amount in dependence of parameters like contact time, nominal composition and surface termination of diamonds. Quantitative analysis of the  $\text{Al}_4\text{C}_3$  amount was performed by gas chromatography. 500 mg of composite material was filled into a 50-mL headspace vial, sealed gas-tight and 15 mL of a 15 wt.-pct. aqueous NaOH solution was added to dissolve Al matrix and  $\text{Al}_4\text{C}_3$  reaction product at ambient temperature and to create gaseous  $\text{CH}_4$ . The gas injection into a Shimadzu GCMS-QP2010 Plus, equipped with a ShinCarbon ST 2 m column of 0.25 mm diameter and 50 m length, was

done manually via a 100-μL gas-tight syringe. The column temperature was held at 313 K for 3 min before it was heated to 453 K at 30 K min<sup>-1</sup> and where it was kept constant for another 2 min. The spectra obtained were analysed using the program GCMS solutions by integrating the significant peaks at the interesting *m/z* ratios. The obtained areas are then used for the quantification of the measured gaseous species. N<sub>2</sub> is used as internal standard, thus the CH<sub>4</sub>/N<sub>2</sub> ratio is proportional to the amounts of Al<sub>4</sub>C<sub>3</sub>. Synthetic Al<sub>4</sub>C<sub>3</sub> (obtained by Alfa Aesar 99 + pct. pure) and pure Al was used for the calibration of the GC-MS system, the corresponding calibration line for the CH<sub>4</sub>/N<sub>2</sub> signal ratios showed a R<sup>2</sup> of 0.995. Residual diamond particles after dissolving the Al(Si) matrix in NaOH were several times rinsed with de-ionized water and ethanol, dried and characterized by SEM.

The microstructure of the composites was prepared by electrochemical etching according to [19]. To illustrate the formation of aluminium carbide at the interface between the matrix and the diamonds as function of different parameters, microstructures and interfaces of the composites were additionally prepared by a ultrashort pulsed Ti/sapphire laser oscillator–amplifier system. It consists of a continuous wave pump laser and a one-level multipass Ti/sapphire amplifier with a kHz pulsed Nd/YLF solid-state pump laser. The used pulse duration of 30 fs at a pulse energy of 0.8 mJ and a repetition rate of 1 kHz ensures a cutting process of minimal thermal interaction. Furthermore, protective He purge gas of 20 L min<sup>-1</sup> was used to suppress formation of aluminium oxides. The samples were mounted onto the rotational axis of a rotary disc and the laser was focused onto the sample. A traversing device with a steady drive was used to cut the samples. Before inspecting the interfaces by SEM the cut specimen surfaces were ion polished by FEI Quanta 200 3D Dual beam system operated with 30 kV Ga<sup>+</sup> ions to remove laser-induced periodic surface structures (LIPSS) artefacts from the laser cutting process.

Applying the Differential Effective Medium (DEM) scheme [20, 21] it is possible to determine the thermal conductance *h* of the aluminium–diamond interface upon fitting the experimental thermal conductivity of each sample. When treating SDB1125 diamond particles as spheres in a first approach, the Differential Effective Medium approach can be used to calculate the composite thermal conductivity  $\kappa_c$  by,

$$(1 - V_i) = \frac{\left(\frac{\kappa_i^{eff}}{\kappa_m}\right) - \left(\frac{\kappa_c}{\kappa_m}\right)}{\left(\frac{\kappa_i^{eff}}{\kappa_m}\right) - 1} \left(\frac{\kappa_c}{\kappa_m}\right)^{-\frac{1}{n}} \tag{2}$$

where  $\kappa_i^{eff}$  the effective, size-dependent thermal conductivity of the inclusion particles (diamonds) in the composite,  $\kappa_m$  that of its matrix and  $V_i$  is the particle volume fraction. In Eq. (2), *n* is the shape factor and assumes to *n* = 3 for spherical particles.

The thermal conductivity of two-phase materials can be predicted by needs to take into account the finite value of the interface thermal conductance between two solid phases, i.e. the inclusion and the encircling matrix in a composite. Analytically, this is typically solved by replacing the inclusion of an intrinsic thermal conductivity  $\kappa_i$  with a non-ideal interface by an “effective” inclusion having an effective conductivity  $\kappa_i^{eff}$  given by

$$\kappa_i^{eff} = \frac{\kappa_i}{1 + \frac{\kappa_i}{ah}} \tag{3}$$

from which *h*, the interface thermal conductance, can be derived by a given inclusion radius *a* [5].

In applying Eqs. (2) and (3), we used the following values of the involved variables: *a* = 190 μm,  $V_i$  = 0.64,  $\kappa_m$  in Table 1 and  $\kappa_i$  = 1740 W m<sup>-1</sup> K<sup>-1</sup>. This given value for  $\kappa_i$  was calculated according to the expression proposed by Yamamoto et al. [22] and by using a concentration of 213 ± 13 ppm of nitrogen, measured by combustion analysis for the SDB1125 diamond particles.

## Results and discussion

### Thermal conductivity and interface thermal conductance

The matrix thermal conductivity  $\kappa_m$  is important to know for the calculation of the interface thermal conductance according to the DEM-model. Table 1

**Table 1** Thermal conductivity of Al and different Al–Si matrix alloys

Si (wt.-pct.)	$\kappa_m$ (W m <sup>-1</sup> K <sup>-1</sup> )
0	235 ± 2
0.5	226 ± 3
1	224 ± 1
3	217 ± 1

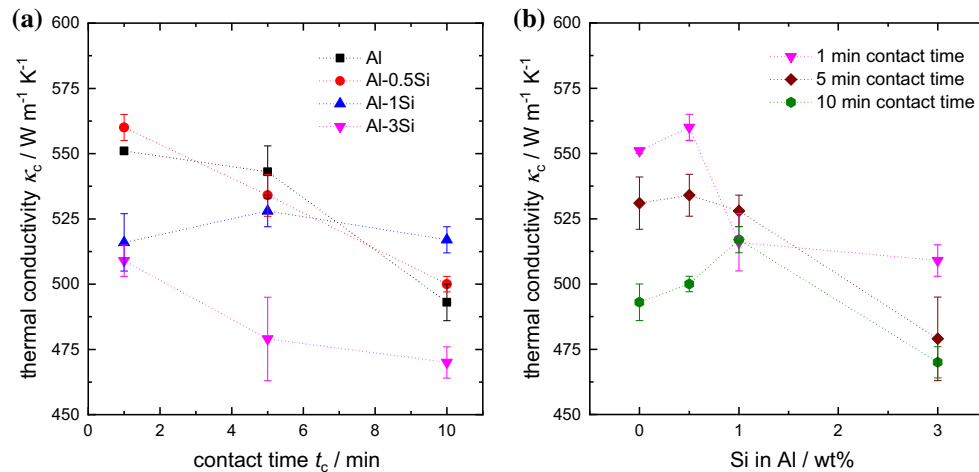


**Figure 1** Composite thermal conductivity  $\kappa_c$  as a function of **a** contact time  $t_c$  between the liquid metal and the as-received diamonds during infiltration, and **b** the Si concentration in Al.

shows that the addition of Si to Al reduces the matrix thermal conductivity  $\kappa_m$  just slightly from  $235 \pm 2$  W m<sup>-1</sup> K<sup>-1</sup> for pure aluminium to  $217 \pm 1$  W m<sup>-1</sup> K<sup>-1</sup> for Al3Si.

Figure 1 displays the influence of the Si concentration in Al from pure Al up to 3 wt.-pct. Si on composite thermal conductivity and 1, 5 and 10 min contact time  $t_c$  between liquid and as-received diamonds during infiltration operation. The data presented are the mean average of three measurements and the error bars correspond to the standard deviation of those measurements. To guide the eyes dotted lines connect the data.

Figure 1a shows an almost linear decrease in thermal conductivity with increasing contact times for all MMCs, except for those with an Al1Si matrix. The MMC based on the Al1Si metal matrix exhibit virtually no influence of the contact time investigated. An increase in the contact time from 1 to 10 min results in a drop of the thermal conductivity of about  $60$  W m<sup>-1</sup> K<sup>-1</sup> for MMCs based on pure Al and Al0.5Si, respectively. Upon an increase in Si in Al to 1 wt.-pct. this decrease diminishes. However, by further addition of Si to the metal matrix to a total amount of 3 wt.-pct. the thermal conductivity drop off due to an increase in the contact time is about  $35$  W m<sup>-1</sup> K<sup>-1</sup>.

Figure 1b shows just another depiction of the data presented in Fig. 1a, but facilitates the recognition of impacts of Si in Al on composite thermal conductivities. There is a general trend for all contact times, that thermal conductivity decreases with increasing

Si in Al, although at low Si (between 0 and 1 wt.-pct.) also an increase in thermal conductivity can be observed for 10 min of contact time, followed by a decrease between 1 and 3 wt.-pct. Si in Al. For contact times of 1 min the addition of Si leads to a reduction in thermal conductivity, when Si in Al is above 0.5 wt.-pct. Upon increasing the contact time to 5 min the differences in the thermal conductivities of the MMCs based on Al, Al0.5Si and Al1Si seem to diminish, while there is still a pronounced drop for Al3Si. A further increase in contact time to 10 min appears to provoke first an increase from pure Al to Al1Si, followed by a severe drop in thermal conductivity for Al3Si, thus rendering the MMC based on an Al1Si matrix the highest thermal conductivity of this series. Again, the Al3Si-based MMC features the lowest measured thermal conductivity.

It is clear, that any additions of Si to Al may lower the intrinsic thermal conductivity of the pure matrix and therefore the thermal conductivity of the respective MMC. The results presented above may be explained, at least partially, by this effect. In particular, this might be true when Si in Al is as low as 0.5 wt.-pct., if we assume that most of the Si keep dissolved in the  $\alpha$ -Al lattice down to ambient temperature. At 1 wt.-pct. Si in Al and during fast cooling,  $\alpha$ -Al solid solution can be supersaturated and then Si can easily precipitate, as the system tends to achieve thermodynamic equilibrium. In a first approach, the thermal conductivity behaviour of Al1Si/diamond may be ascribable to the contribution



of thermally high conductive precipitated Si particles in the Al–Si matrix.

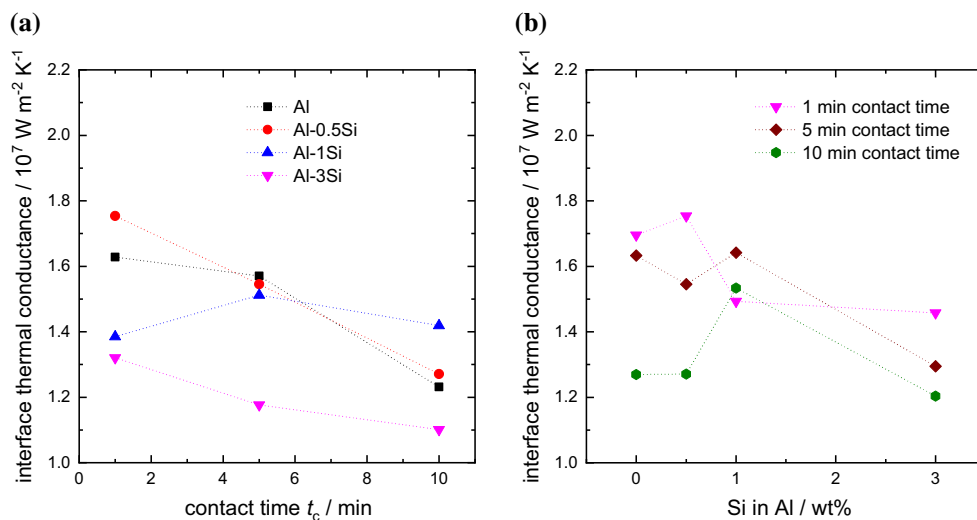
This should be true as well for Al<sub>0.5</sub>Si alloys, but supersaturation is much lower and Si may not precipitate due to kinetic inhibition, thus the impact on thermal composite conductivity is lower or even negligible. This, however, may not fully explain the relatively independent thermal conductivity behaviour of Al<sub>1</sub>Si/diamond MMCs with respect to contact time or the increase in conductivity for Al<sub>0.5</sub>Si/diamond and Al<sub>1</sub>Si/diamond with respect to pure Al/diamond and Al<sub>3</sub>Si/diamond at contact time of 10 min. The formation or suppression of Al<sub>4</sub>C<sub>3</sub> with contact time and Si in Al may be decisive as well (see below). For two-phase matrix compositions above the maximum solubility of Si in  $\alpha$ -Al of 1.65 wt.-pct. [23], (almost) pure Si is formed during solidification by eutectic reaction. As the Al<sub>3</sub>Si alloy contains roughly three vol.-pct. Si particles, the thermal conductivity will be reduced by some 7.5 pct. (see Table 1). Again, this may not fully explain the thermal conductivity behaviour of Al<sub>3</sub>Si/diamond composites.

Figure 2a, b plots the calculated interfacial thermal conductance in applying Eqs. (2) and (3) and the data in Table 1 as a function of contact time and Si in Al, respectively. Not surprisingly, those graphs indicate a comparable trend to the thermal conductivity graphs in Fig. 1. That is a general trend of decreasing ITC with increasing contact time, except for Al<sub>1</sub>Si/diamond MMCs, the lowest ITC for

Al<sub>3</sub>Si/diamond MMCs in all investigated contact times, and the highest ITC values for pure Al/diamond and Al<sub>0.5</sub>Si/diamond at 1 min contact time (Fig. 2a). Furthermore, upon increasing Si in Al at 1 min contact time the ITC significantly decreases at Si concentrations higher than 0.5 wt.-pct., although it then appears to be constant up to 3 wt.-pct. At a contact time of 5 min this decrease in ITC is shift to > 1 wt.-pct. Si in Al. At 10 min the ITC is lowest for pure Al/diamond and Al<sub>0.5</sub>Si/diamond and highest for Al<sub>1</sub>Si/diamond, followed by a significant decrease in ITC upon approaching 3 wt.-pct. Si in Al (Fig. 2b). Again, Al<sub>1</sub>Si appears to be the most convenient matrix composition when aiming for a maximum ITC that should be independent of processing conditions.

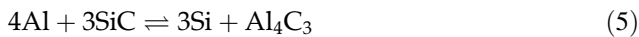
### Formation of interfacial carbides

To shed some light on the thermal conductivity results, the formation of Al<sub>4</sub>C<sub>3</sub> in dependence of Si in Al and contact time has to be discussed in detail. In a general notion, any increase in contact time between the molten metal and the diamond particles may result in increased formation of interfacial Al<sub>4</sub>C<sub>3</sub>, as qualitatively shown in a previous study by Monje et al. [18]. Nearby, the formation of Al<sub>4</sub>C<sub>3</sub> is preceded by the dissolution of carbon from diamond surface and the diffusion of carbon through the liquid Al [6], furthermore, reactivity appears to be distinct for the different diamond faces [7].



**Figure 2** Interface thermal conductance as a function of **a** contact time  $t_c$  between the liquid metal and the as-received diamonds during infiltration, and **b** the Si concentration in Al.

Furthermore, it is known from previous studies that the addition of Si to Al may effectively suppress the formation of  $\text{Al}_4\text{C}_3$  by the preferential formation of SiC [Eq. (4)]. However, it is also possible, that by subsequent reaction, some (“pure”) Si and  $\text{Al}_4\text{SiC}_4$  phases, respectively, can be generated according to Eqs. (5) and (6):



The kinetic evolution of interfacial  $\text{Al}_4\text{C}_3$  formation during processing of Al/diamond MMCs can be discussed by means of a quantitative evaluation of the GC–MS results. Figure 3a indicates an increase in  $\text{Al}_4\text{C}_3$  concentration with contact time for all MMCs, with the highest slope for pure Al/diamond and the highest concentration of  $\text{Al}_4\text{C}_3$  of 4.14 wt.-pct. at a contact time of 10 min. For Al0.5Si, Al1Si and Al3Si-MMCs, the increase in  $\text{Al}_4\text{C}_3$  with increasing contact time is significantly smaller than in pure Al/diamond. Differences in  $\text{Al}_4\text{C}_3$  between Al0.5Si/diamond and Al1Si/diamond appear to be almost negligible, interestingly  $\text{Al}_4\text{C}_3$  concentrations in Al3Si/diamond are higher than the before mentioned two MMCs with matrix alloys Al0.5Si and Al1Si.

At a contact time of 1 min the  $\text{Al}_4\text{C}_3$  concentration appears to be almost independent of Si concentration in Al (Fig. 3b). At contact times of 5 and 10 min, the concentration of interfacial  $\text{Al}_4\text{C}_3$  can be significantly reduced by the addition of as small concentration as 0.5 wt.-pct. Si in Al. Upon further increasing the Si in

Al concentration, this effect almost diminishes or appears to result in an even slight increase in  $\text{Al}_4\text{C}_3$ . We conclude first that the formation of  $\text{Al}_4\text{C}_3$  is effectively suppressed by the addition of small amount of Si to Al and, second, sort of “equilibrium” amount of  $\text{Al}_4\text{C}_3$  is presently uncoupled from Si concentrations, solely depending on contact times. The largest decrease in  $\text{Al}_4\text{C}_3$  from 4.14 to 2.78 wt.-pct., i.e. one-third of the initial concentration, can be observed at 10 min contact time by the addition of 0.5 wt.-pct. Si to Al. At a contact time of 5 min, this decrease is in the same order of magnitude, i.e. about 28 pct of the initial interfacial carbide concentration. For contact time of 1 min the formation of interfacial carbides appears to be almost independent of Si in Al, with a tendency to a negligible increase from 1.76 to 1.84 wt.-pct. between pure Al and Al3Si (Fig. 3b).

As discussed above, the increase in  $\text{Al}_4\text{C}_3$  with increasing contact times is almost the same for all MMCs with Al–Si matrices, suggesting a similar growth mechanism whenever Si is present in the diamond MMCs. Hence, the results of the GC–MS measurements helped towards an explanation for the steady decrease in thermal conductivity with increasing contact time, as excessive formation of interfacial carbide is supposed to strongly limit the thermal transport across the diamond–metal interface [18, 24]. However, the fact that Al3Si-based MMCs possess lower thermal conductivities than pure Al MMCs for all contact times, although featuring significantly lower amounts of  $\text{Al}_4\text{C}_3$ , and the independence in thermal conductivity of Al1Si-based MMCs

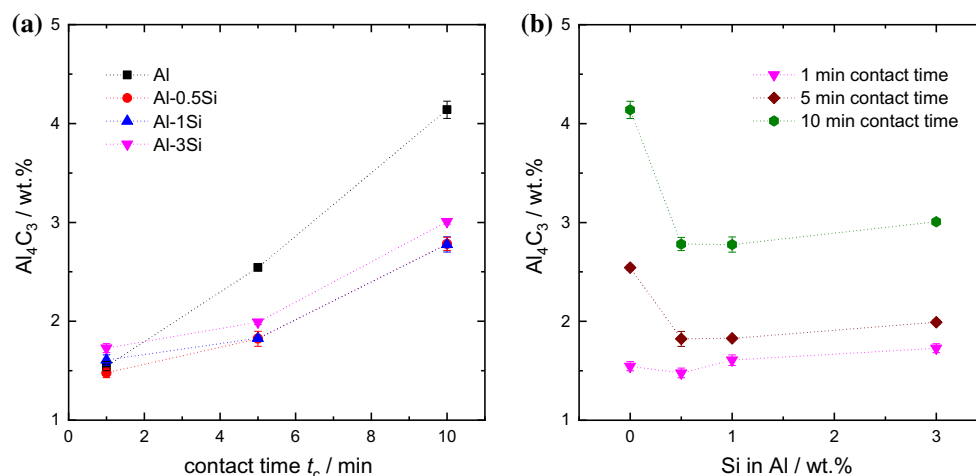


**Figure 3** Concentration of  $\text{Al}_4\text{C}_3$  as a function of contact time  $t_c$  between the liquid metal and the as-received diamonds during infiltration (a) and the Si concentration in Al (b).

on all contact times need further contemplation, for which reasons the microstructures of the corresponding MMCs were observed (see “Materials microstructure” section).

### Surface termination

Before considering microstructural investigations, the impact of diamond surface termination on thermal conductivity behaviour and interfacial carbide formation has to be discussed as well. Figure 4 displays the composite conductivity  $\kappa_c$  as a function of Si in Al concentration and diamond surface termination for different contact times. An impact of O-termination on composite thermal conductivity, i.e. an increase compared to the H-terminated and the as-received diamonds, is visible for almost all investigated contact times and different matrix compositions. In general, the H-terminated diamond surfaces exhibit the lowest  $\kappa_c$  of all investigated MMCs, with the most distinct decline of approx. 20 pct. for a contact time of 10 min and 3 wt.-pct. of Si in Al (Fig. 4c) compared to the  $\kappa_c$  of the materials using the as-received and those using the O-terminated diamonds.

Interestingly, the interfacial carbide concentration in Fig. 5 appears to be (at least partially) decoupled from the thermal conductivity behaviour in Fig. 4. At a contact time of 1 min the  $\text{Al}_4\text{C}_3$  concentration for pure Al/diamond, Al0.5Si/diamond and Al1Si/diamond is very low and apparently independent of surface termination, whereas the thermal conductivity differs with respect to the surface termination. For Al3Si/diamond, the interfacial carbide concentration is different for the dissimilar surface terminations,

interestingly lowest for the H-terminated diamonds and highest for O-termination (Fig. 5a). We conclude that at contact times of 1 min surface termination has a minor influence on the formation of  $\text{Al}_4\text{C}_3$ , but  $\kappa_c$  is affected by the diamond surface termination for matrix compositions of  $\leq 1$  wt.-pct. Si in Al.

At a contact time of 5 min, Fig. 5b,  $\text{Al}_4\text{C}_3$  concentration is highest for pure Al/diamond and decreases upon adding 0.5 wt.-pct. Si to Al, independently of surface termination. Any further increase in Si has no further effect on the formation of interfacial carbides, whether diamonds are surface terminated or not. This is again in contradiction to the composite thermal conductivity behaviour, Fig. 4b, as O-termination results in an increase in  $\kappa_c$  compared to the as-received and the H-terminated diamonds. For  $t_c$  of 10 min (Fig. 5c) the same behaviour can be identified upon adding Si to Al, as the interfacial carbide concentration is highest for pure Al/diamond and significantly decreases upon adding 0.5 wt.-pct. of Si to Al. Interestingly, at  $t_c = 10$  min the H-terminated diamond MMCs feature the lowest concentration of formed  $\text{Al}_4\text{C}_3$  for all matrix compositions in this series. Composites using as-received diamond and O-terminated ones show a significant higher concentration in interfacial carbides, independently of the nominal matrix composition. However, the very high  $\text{Al}_4\text{C}_3$  concentration close to 4 wt.-pct. for all pure Al/diamond at  $t_c = 10$  min results in the lowest composite thermal conductivities in this series. It is furthermore interesting to identify, that the low  $\text{Al}_4\text{C}_3$  concentration in H-terminated Al3Si/diamond MMC at  $t_c = 10$  min does not result in a higher  $\kappa_c$  compared to the two other MMCs in this series, as both exhibit a

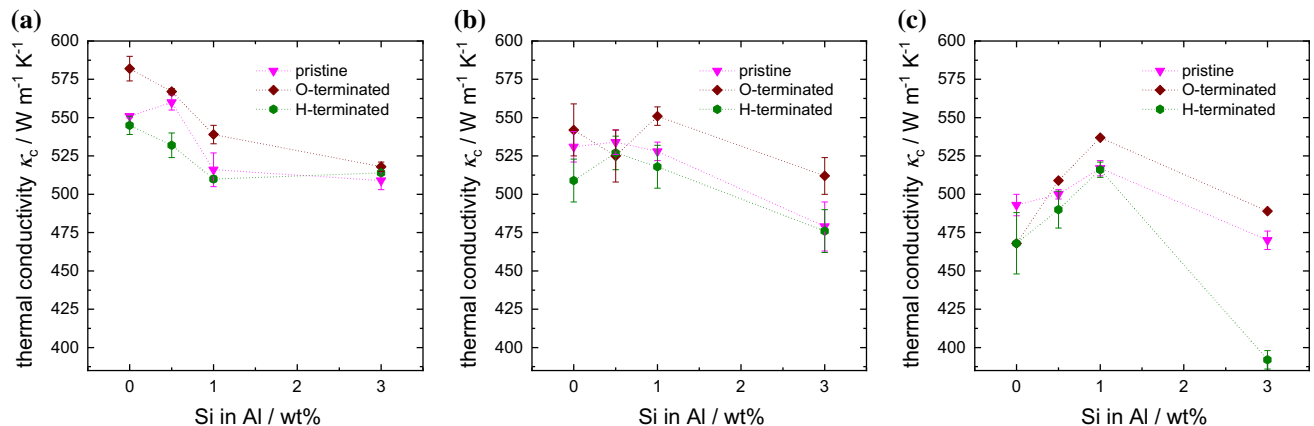


**Figure 4** Composite thermal conductivity  $\kappa_c$  as a function of Si concentration in Al at **a** 1 min, **b** 5 min and **c** 10 min contact time  $t_c$  between the liquid metal and as-received (“pristine”), O-terminated and H-terminated diamonds.



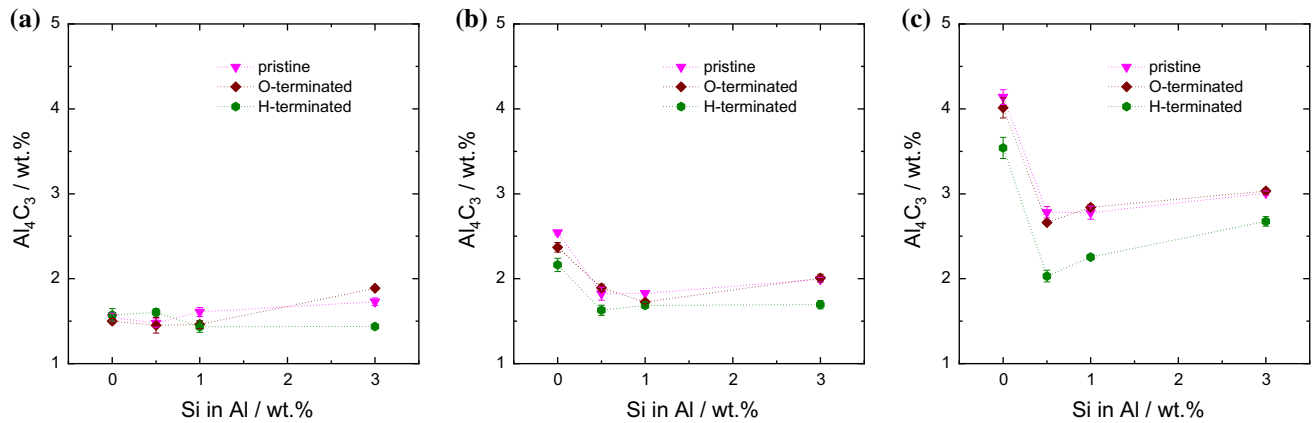


**Figure 5** Concentration of  $\text{Al}_4\text{C}_3$  as a function of Si concentration in Al at **a** 1 min, **b** 5 min and **c** 10 min contact time  $t_c$  between the liquid metal and as-received (“pristine”), O-terminated and H-terminated diamonds.

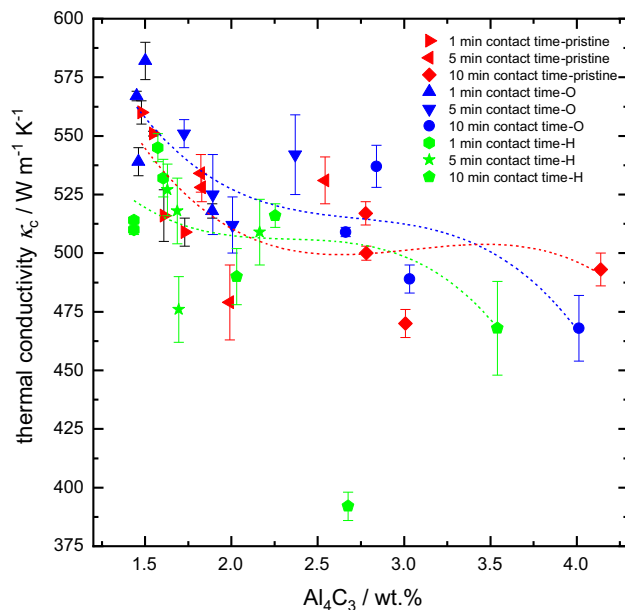


**Figure 6** Composite thermal conductivity  $\kappa_c$  as a function of  $\text{Al}_4\text{C}_3$  concentration and diamond surface termination. The dotted lines represent the polynomial fits of data associated with the respective different surface terminations.

higher interfacial carbide concentration and a higher  $\kappa_c$ .

Figure 6 shows a consistency check for the relationship between composite thermal conductivity and interfacial carbide concentration in dependence of processing conditions contact time and surface termination. As expected, there is a general trend towards lower composite conductivities for higher carbide concentrations. It is also clear, that contact time and surface termination play its role, as for the

same carbide concentration the conductivity can be different.

In a first approach one may expect that the amount—and thus the size—of the interfacial carbide layer will decrease the overall composite thermal conductivity  $\kappa_c$ , as the intrinsic thermal property of  $\text{Al}_4\text{C}_3$  is poor and can be considered as an additional thermal barrier for thermal transport and coupling between electrons and phonons across dissimilar materials at interfaces. Considering above results we conclude, that termination of diamonds surfaces additionally either affects the microstructure (see “Materials microstructure” section) or has a major impact on bonding strength between diamonds and the matrix, thus influencing the thermal transport irrespective from interfacial carbide growth. This conclusion might also hold as in the findings of Monachon [25] the authors argue for the presence of monolayer of oxygen in Al/O that changes the way heat passes through the interface between sputtered Al layer and large diamond mono-crystals by creating Al/O interfacial states. In previous findings of the same authors [10] the interface thermal conductance in a “clean model system” of H-terminated diamond surfaces with a sputtered Al layer is substantially lower compared to O-terminated diamond surface. Furthermore, XPS spectra showed that the proportion of C–O bond drastically increases upon Ar/O plasma treatment as well as acid treatment. Both treatments seemed to be linked positively to a C–O surface termination, though it could also be due to the absence of surface hydrogen since pure Ar plasma treatments led to similar values. Furthermore, Qi and Hector [26, 27] and Wang et al. [28] investigated interfacial

bonding strength between Cu/diamond and Al/diamond, respectively, by first-principle calculations. They found that there is a significant decrease in calculated work of separation values upon introducing H-termination at the clean diamond surface. Electronic structure analysis showed strong covalent bonding between Al and C, but no bonds exist between Al and the H-passivated diamond surface, thus responsible for weak interfacial strength.

**Materials microstructure**

Figure 7 clearly indicates a significant amount of  $Al_4C_3$  crystals present on both diamond faces at a contact time of 1 min for pure Al/diamond. Apparently, our fabrication conditions, in particular the infiltration temperature of 1173 K, are favouring the formation of  $Al_4C_3$  at this low contact times, which is in contrast to the magnitude of occupancy with

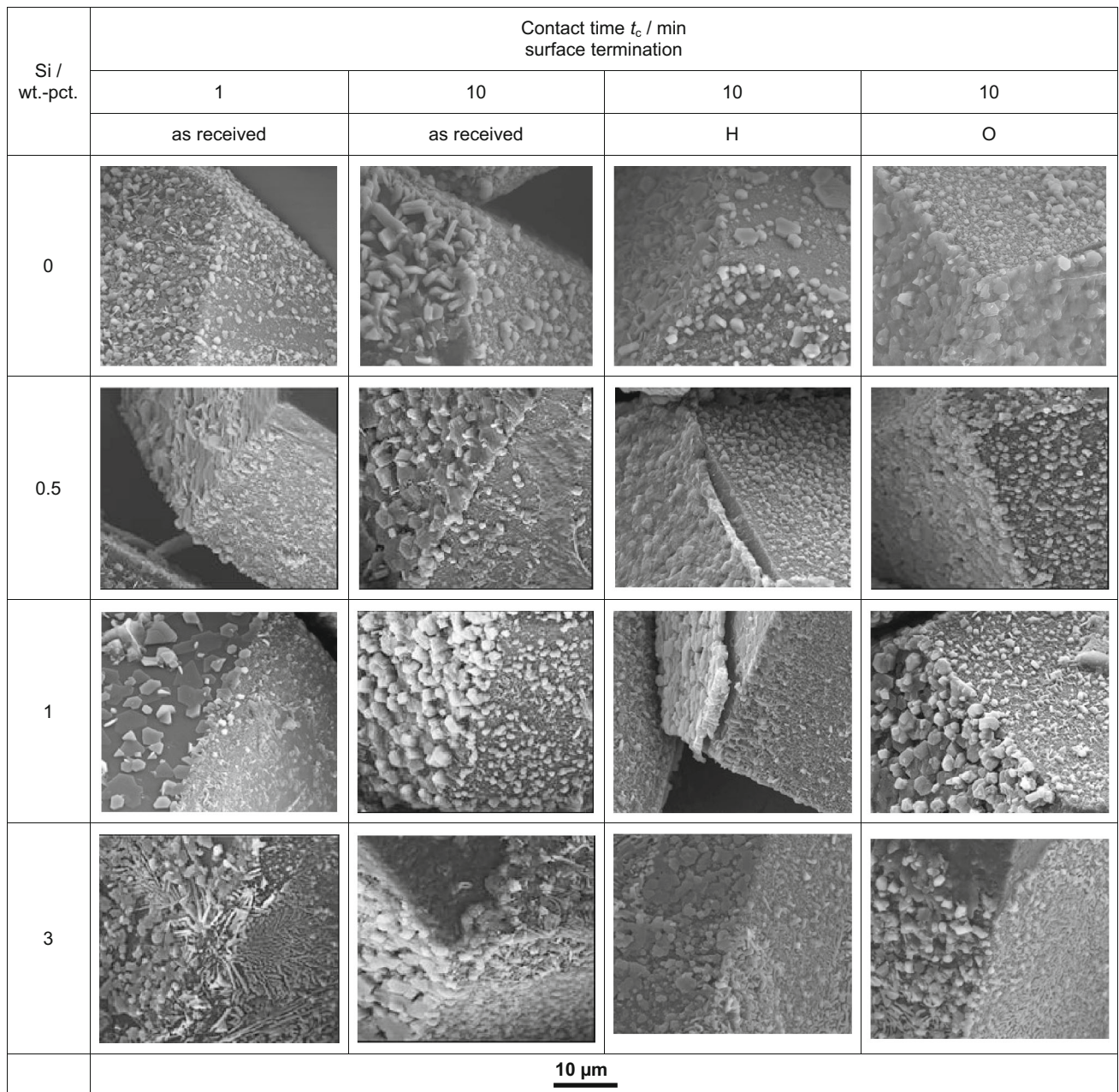


**Figure 7** SE-images showing the microstructures of selected MMCs, prepared by electrochemical etching. The left-hand side in each of the images corresponds to the (111) diamond face and the right-hand side always displays the (100) face.

interfacial carbides on diamond faces in the study of Monje et al. [18]. This might be attributed to the 50 K higher infiltration temperature in our investigations, or may be due to additional processing parameters, that cannot be exactly defined now. Moreover, an increase in contact time to 10 min results in significantly larger  $\text{Al}_4\text{C}_3$  crystals.

The interfacial  $\text{Al}_4\text{C}_3$  microstructure in  $\text{Al}_{10.5}\text{Si}$ /diamond MMCs is quite similar to pure Al/diamond. For  $\text{Al}_{11}\text{Si}$ /diamond MMCs this microstructure is obviously different to pure Al/diamond already at a contact time of 1 min, as the  $\text{Al}_4\text{C}_3$  crystals present at the (111) face appear to be larger and more regular in shape. However, the diamonds surface appears to be less covered by the  $\text{Al}_4\text{C}_3$  phase. Also, the (100) diamond face seems to feature less amounts of  $\text{Al}_4\text{C}_3$  compared to the one of pure Al/diamond and exhibit very tiny crystals that might be Si or SiC. Upon increasing the contact time to 10 min the interfacial carbides grow again in size and tend to fully cover both crystallographic diamond faces.

By comparing the microstructures of Al- and  $\text{Al}_{11}\text{Si}$ -based MMCs produced with a contact time of 10 min it is evident, that the growth of the  $\text{Al}_4\text{C}_3$  crystals is reduced upon the addition of Si. In particular, the  $\text{Al}_4\text{C}_3$  crystals on the (111) diamond surface are much smaller. This observation is also fortified by the GC–MS measurements, as decreasing  $\text{Al}_4\text{C}_3$  amounts were detected for  $\text{Al}_{11}\text{Si}$ /diamond. Hence it may be concluded, that a uniform coverage of the diamond surface by  $\text{Al}_4\text{C}_3$  may be desirable, as the thermal conductivity increased by increasing the contact time to 5 min. The limitation of the  $\text{Al}_4\text{C}_3$  growth by the addition of Si aids towards thermal conductivities that are rather unaffected by the chosen contact times. The microstructures of the  $\text{Al}_{13}\text{Si}$ -based MMCs, however, show a significantly different appearance than the ones observed before, as now spicular, Si-enriched crystals appear on both crystallographic diamond orientations. Moreover, the (100) diamond surface appears to be more covered by those crystals than the (111) faces. According to Eqs. (4)–(6) these phases can be either Si (moreover, Si crystals may also be present due to the eutectic reaction between Al and Si upon solidification), SiC and  $\text{Al}_4\text{SiC}_4$ , respectively. In fact, the spicular phases visible in Fig. 7 could not be clearly identified and assigned to an accurate compound by XRD, as their amounts are too small for correct identification. Anyhow, it

sometimes appears that these Si containing crystals grow on top or in between the  $\text{Al}_4\text{C}_3$  layer.

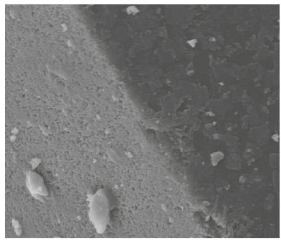
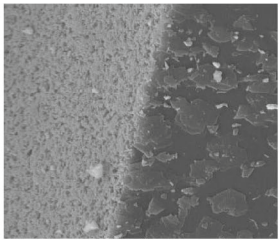
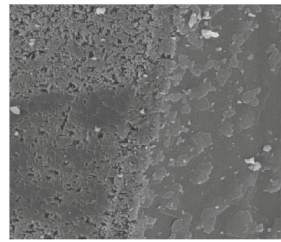
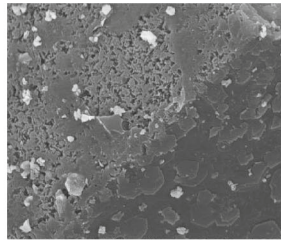
By comparing the microstructures of  $\text{Al}_{13}\text{Si}$ -based MMCs produced with 1 and 10 min contact time, it can be seen that the  $\text{Al}_4\text{C}_3$  crystals again grow in size (and perhaps also in thickness) when contact time increases. Once again, this statement is confirmed by quantitative analysis, as the  $\text{Al}_4\text{C}_3$  concentration increases with contact time (Fig. 3a), but with a much smaller slope upon the further addition of Si to Al (Fig. 3b). These Si-enriched crystals now also aid towards an explanation of the thermal conductivities of the  $\text{Al}_{13}\text{Si}$ -based MMCs: since these phases act as an additional barrier in the thermal transport across the diamond/ $\text{Al}_4\text{C}_3$ /metal interface, in addition to a reduction in intrinsic matrix conductivity (Table 1). Additionally, the thermal conductivities of the  $\text{Al}_{13}\text{Si}$ -based MMCs appear to be influenced again by contact time, which seemingly can be explained by the increase in  $\text{Al}_4\text{C}_3$  concentration with increasing contact time.

When comparing oxygenated and hydrogenated diamond surfaces with as-received ones it is evident that H-termination obviously results in delaminated  $\text{Al}_4\text{C}_3$  layer due to weak bonds between the interlayers and the (111) diamond faces in  $\text{Al}_{10.5}\text{Si}$ /diamond and  $\text{Al}_{11}\text{Si}$ /diamond composites. The presence of high concentration of Si in  $\text{Al}_{13}\text{Si}$ /diamond may force bonding even for H-terminated surfaces, thus, delamination is suppressed. Interestingly, any difference between oxygenated and as-received diamond surfaces appears to be negligible, size and thickness of interlayers are comparable.

Residual diamonds from the GC–MS investigations can be also used to study reactivity between Al matrix and diamonds, as shown in Fig. 8. For  $\text{Al}_{13}\text{Si}$ /diamond MMCs, interestingly, the (111) diamond faces show very small dimples originating from the dissolution of carbon (diamond) by the reaction with liquid Al, whereas the (100) faces show a rather smooth surface topography with no dimples but sort of a replica of the previously large and blocky, plate-like  $\text{Al}_4\text{C}_3$  crystals at those faces. There is obviously no difference in dimples visible between specimens of different contact times and surface terminations.

Three samples were selected to be prepared by laser cutting: two Al-based ones with contact times of 1 and 10 min and one  $\text{Al}_{13}\text{Si}$ /diamond with a contact time of 10 min (all with as-received diamonds).



Si / wt.-pct.	Contact time $t_c$ / min surface termination			
	1	10	10	10
	as received	as received	H	O
3				
	<b>10 <math>\mu</math>m</b>			

**Figure 8** SE-images showing the microstructures of selected diamonds, extracted by dissolution of Al<sub>3</sub>Si/diamond MMCs in NaOH (during GC–MS investigations). The left-hand side in each

of the images corresponds to the (111) diamond face and the right-hand side always displays the (100) face.

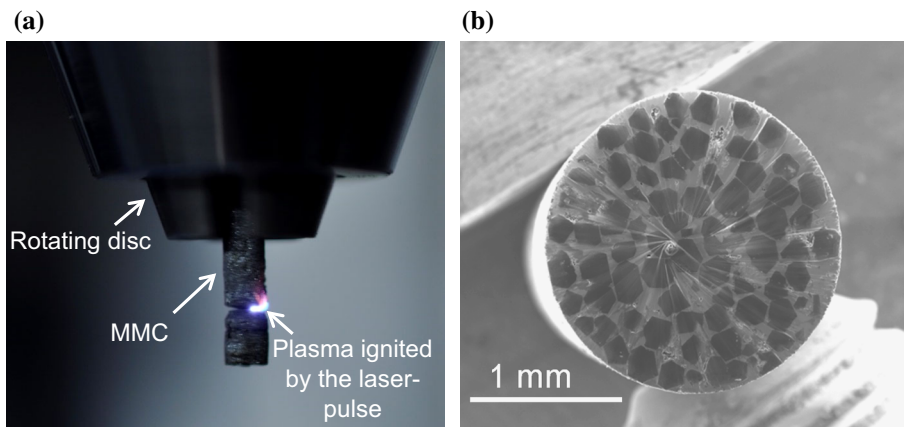


**Figure 9** Monitoring cutting process of Al/diamond MMC by fs laser (a) and cross section after finishing cutting (b).

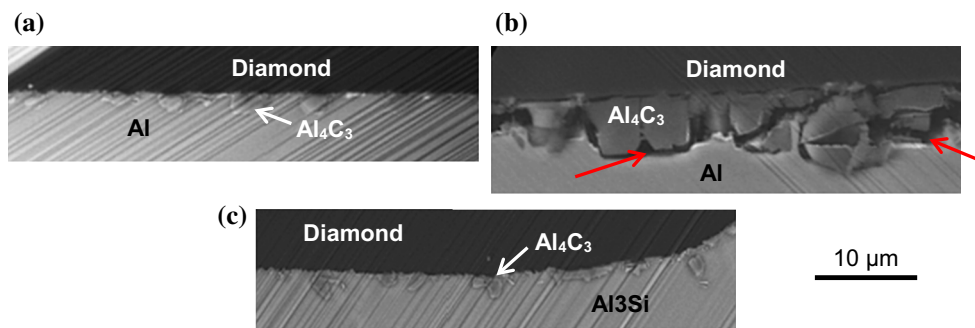


**Figure 10** Laser-cut cross sections of Al/diamond MMCs with as-received diamonds at **a** 1 min and **b** 10 min contact time and **c** Al<sub>3</sub>Si/diamond at 10 min contact time.

**Table 2** Interfacial layer thickness of selected MMCs

Si (wt.-pct.)	Contact time $t_c$ (min)	Interfacial carbide layer thickness ( $\mu\text{m}$ )
0	1	0.3–2.2
0	10	4.4–9.1
3	10	0.4–2.5

Figure 9a displays the experimental arrangement of laser cutting process while processing, and Fig. 9b gives the cross section after the laser cutting process, indicating a smooth surface.

The respective BSE-images of the cross sections are shown in Fig. 10. Note, that the parallel lines visible in each of the images are residual artefacts (LIPSS, i.e. laser-induced periodic surface structures) from the laser cutting procedure. Although subsequent ion polishing drastically reduces LIPSS, they cannot be fully avoided.

An interfacial compound with intermediate grey scale can be identified at each metal-diamond interface and which is most probably  $\text{Al}_4\text{C}_3$ . The  $\text{Al}_4\text{C}_3$  compound does not grow layer like, but rather as large individual crystals, as already supposed by the images of the electrochemically prepared samples in Fig. 7. It can be seen that upon an increase in contact time from 1 to 10 min a significant increase in layer thickness takes place. An average layer thickness of the  $\text{Al}_4\text{C}_3$  interfacial compound was determined from image analysis, as shown in Table 2.

The interfacial layer thickness increases from 0.3–2.2  $\mu\text{m}$  at 1 min contact time to 4.4–9.1  $\mu\text{m}$  at 10 min. Furthermore, a clear delamination of the  $\text{Al}_4\text{C}_3$  “layer” can be seen, as significant amounts of voids are visible and highlighted by arrows in Fig. 10b. Upon the addition of 3 wt.-pct. Si to Al the formation of  $\text{Al}_4\text{C}_3$  appears to be strongly hampered, as the cut cross section is similar to the pure Al-based MMC with 1 min contact time. This average thickness of the interfacial carbide layer was determined to be between 0.4 and 2.5  $\mu\text{m}$ . Therefore, the statement made above, that Si limits the interfacial  $\text{Al}_4\text{C}_3$  growth (in thickness) is confirmed.

In order to complete the picture how Si in Al limits the  $\text{Al}_4\text{C}_3$  growth, EDX-mapping and line scans (not displayed) were performed at the metal/diamond interface of a laser-cut cross section in an Al3Si/diamond specimen (Fig. 11). Interestingly, Si accumulates near this interface in the small-scaled  $\text{Al}_4\text{C}_3$

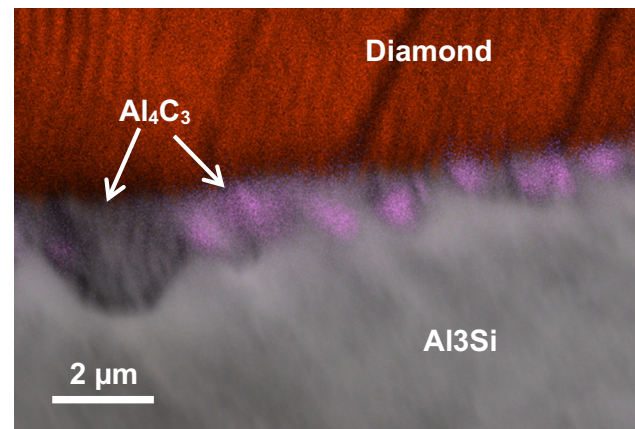


**Figure 11** Elemental mapping of the laser-cut cross section area of Al3Si-based MMC with as-received diamonds at contact time of 10 min, element overlay images of Si K (magenta), C K (brown) and Al K (grey).

crystals, whereas in the larger  $\text{Al}_4\text{C}_3$  crystal no or very minor amounts of Si are detected (Fig. 11). Hence, such interfacial Si accumulations imply that most probably a phase like  $\text{Al}_4\text{SiC}_4$  (Eq. 6) or even Si and SiC (Eqs. 4, 5) in closely spaced areas with  $\text{Al}_4\text{C}_3$  are formed that govern the kinetics of interfacial  $\text{Al}_4\text{C}_3$  growth in Al3Si/diamond. However, the formation of such compounds remains to be clarified. Detection of very small amounts of oxygen can be attributed to the oxidation of the sensitive interfacial carbides, rather than the presence of  $\text{Al}_2\text{O}_3$  layers, that will also influence interfacial thermal transport [25].

In quantitative spot and line analysis, the amounts of Si detected ranged from 0.88 wt.-pct. (close to the matrix) to 7.49 wt.-pct. (within the interfacial carbides). Therefore, Si concentrations that are almost 9 times higher than the Si in the matrix are quantified inside the interfacial layers. However, it is still possible that a very small SiC film (perhaps in the order of few nanometres) forms at the interface, also limiting the growth of  $\text{Al}_4\text{C}_3$ , since the detection limit of the SEM is comparably bad and co-quantification of carbon (from diamond) occurs. Ruch et al. [6] also noticed Si at the diamond/matrix interface after processing, but no formation of SiC in Al7Si/diamond MMCs, although thermodynamically feasible. They also argued that the solubility of carbon in liquid aluminium is limited by addition of Si and which leads to reduced capability to form  $\text{Al}_4\text{C}_3$  at given temperatures and processing times by reducing the contact cross section between aluminium and



diamond [29]. Beffort et al. [30] investigated the Al7Si/diamond system processed by gas pressure assisted infiltration and observed a 50–200-nm-thick amorphous interface layer. Accompanying line scans revealed C, Al, O and a very small signal of Si, close to the diamond surface. The authors further concluded that this amorphous layer is most probably catalyzed by the contact with the Al(Si) melt. Element partitioning within the amorphous interface layer appeared to be responsible for enhanced interfacial bonding between the diamond and the matrix, as they furthermore found imprints of the eutectic skeleton of Si on the surface of the torn-out diamond surfaces. This presence of Si skeleton also may be responsible for the absence of carbide formation.

This, however, will not fully explain the observed enrichment of Si in the interfacial carbide region in the present work. Including our findings we may argue for the existence of Al–Si–C phases at the interface like  $\text{Al}_4\text{SiC}_4$  that have an impeded smaller rate of growth compared to  $\text{Al}_4\text{C}_3$  in pure Al/diamond, with the later having an unimpeded growth of interfacial carbides.

## Conclusion

In this study, we investigated chemical analysis and thermal properties of Al(Si)/diamond composites and the influence of processing conditions, nominal matrix composition and surface termination of diamonds on interfacial carbide formation, and it has been shown that:

- Both contact time and Si concentration in the Al matrix have a major impact on the thermal conductivity behaviour of the corresponding MMCs. For a pure Al and Al0.5Si matrices, the thermal conductivities of the respective MMCs decrease almost linearly with increasing contact time. The same behaviour, although to a lessened amount, are found for the MMCs based on Al3Si. The MMCs with an Al1Si matrix, however, showed virtually no influence of the contact time on the thermal conductivities observed.
- This behaviour could be explained by the steady growth of interfacial  $\text{Al}_4\text{C}_3$ , as observed in the GC–MS measurements, as the addition of Si to the Al matrix limits the formation of  $\text{Al}_4\text{C}_3$ . In addition, the microstructures, prepared by electrochemical etching of the MMCs showed increasing size of  $\text{Al}_4\text{C}_3$  crystals with increasing contact time. Again, the addition of Si appears to limit this growth. The microstructure of the Al3Si-based MMC featured additional Si-enriched components on top of or in confined areas with  $\text{Al}_4\text{C}_3$  crystals, which may be a part of eutectic Si phase or Al–Si–C phase and which are believed to decrease the thermal conductivities of the corresponding MMCs.
- Considering quantitative results for  $\text{Al}_4\text{C}_3$  together with the thermophysical behaviour described in “Thermal conductivity and interface thermal conductance” section, Al1Si/diamond appears to be an interesting matrix composition, as both ITC and  $\text{Al}_4\text{C}_3$  appear to be quite independent of processing conditions. In a first approach, this might be attributed to an optimum balanced proportion between “precipitated” Si phase of high intrinsic thermal conductivity (respectively, a minor amount of dissolved Si in the  $\alpha$ -Al lattice), that may facilitate strong bonding between the diamond particles and the Al matrix and the suppression of excessive formation of  $\text{Al}_4\text{C}_3$ .
- Surface termination positively affects composite thermal conductivity as oxygenated diamond surfaces will result in an increase in  $\kappa_c$ . Interestingly, surface termination plays a minor role in the formation of  $\text{Al}_4\text{C}_3$  at low Si in Al and contact times of 1 min. At 5 and 10 min contact time, the H-termination results in a decline of  $\text{Al}_4\text{C}_3$  formation for all investigated matrix compositions. Composites using as-received diamond and O-terminated ones show a higher concentration in interfacial carbides, independently of the nominal matrix composition. It is most likely that the concentration of  $\text{Al}_4\text{C}_3$  has no direct impact on the composite thermal conductivity at contact times of 5 and 10 min. We furthermore conclude that termination of diamonds surfaces strongly affects the bonding strength between diamonds and the matrix, thus enhancing the thermal transport irrespective of interfacial carbide growth.
- Microstructural investigations show that hydrogenated diamond surfaces obviously result in delaminated  $\text{Al}_4\text{C}_3$  layer due to weak bonds between the interlayers and the (111) diamond faces in Al0.5Si/diamond and Al1Si/diamond composites. The presence of high concentration

of Si in Al<sub>3</sub>Si/diamond may force bonding even for H-terminated surfaces, thus, delamination is suppressed. Interestingly, any microstructural difference between oxygenated and as-received diamond surfaces appears to be negligible, size and thickness of interlayers are comparable.

- The interface between matrix and diamonds was successfully prepared by laser cutting, thus enabling the study of growth and size of the carbides with process parameters. Furthermore, EDX-mapping clearly showed that Si—present in Al<sub>3</sub>Si matrix alloys—is accumulated in the interfacial layer. We conclude that Si-rich phases are responsible for limiting the size of the interlayer.

## Acknowledgements

Open access funding provided by TU Wien (TUW).

## Compliance with ethical standards

**Conflict of interest** The authors declare that they have no conflict of interest.

**Open Access** This article is distributed under the terms of the Creative Commons Attribution 4.0 International License (<http://creativecommons.org/licenses/by/4.0/>), which permits unrestricted use, distribution, and reproduction in any medium, provided you give appropriate credit to the original author(s) and the source, provide a link to the Creative Commons license, and indicate if changes were made.

## References

- [1] Naidich YV, Kolesnichenko GA (1964) Study of the wetting of diamond and graphite by liquid metals. *Powder Metall Met Ceram* 2:35–38
- [2] Scott PM, Nicholas M, Dewar B (1975) The wetting and bonding of diamonds by copper-base binary alloys. *J Mater Sci* 10:1833–1840. <https://doi.org/10.1007/BF00754470>
- [3] Schubert T, Trindade B, Weißgärber T, Kieback B (2008) Interfacial design of Cu-based composites prepared by powder metallurgy for heat sink applications. *Mater Sci Eng A* 475:39–44
- [4] Neubauer E, Kladler G, Eisenmenger-Sittner C, Hell J, Prentice C, Angerer P, Ciupinski L (2009) Interface design in copper-diamond composite by using PVD and CVD coated diamonds. *Adv Mater Res* 59:214–219
- [5] Tavangar R, Molina JM, Weber L (2007) Assessing predictive schemes for thermal conductivity against diamond-reinforced silver matrix composites at intermediate phase contrast. *Scr Mater* 56:357–360
- [6] Ruch PW, Beffort O, Kleiner S, Weber L, Uggowitzer PJ (2006) Selective interfacial bonding in Al(Si)-diamond composites and its effect on thermal conductivity. *Compos Sci Technol* 66:2677–2685
- [7] Kleiner S, Khalid FA, Ruch PW, Meier S, Beffort O (2006) Effect of diamond crystallographic orientation on dissolution and carbide formation in contact with liquid aluminium. *Scr Mater* 55:291–294
- [8] Beffort O, Vaucher S, Khalid FA (2004) On the thermal and chemical stability of diamond during processing of Al/diamond composites by liquid metal infiltration (squeeze casting). *Diam Relat Mater* 13:1834–1843
- [9] Simancik F, Jangg G, Degischer HP (1993) Short carbon fiber-aluminium matrix composite material prepared by extrusion of powder mixtures. *J Phys IV France* 03:C7-1775–C7-1780
- [10] Monachon C, Weber L (2013) Influence of diamond surface termination on thermal boundary conductance between Al and diamond. *J Appl Phys* 113:183504
- [11] Collins KC, Chen S, Chen G (2010) Effects of surface chemistry on thermal conductance at aluminum–diamond interfaces. *Appl Phys Lett* 97:083102
- [12] Monachon C, Weber L (2012) Thermal boundary conductance of transition metals on diamond. *Emerg Mater Res* 1:89–98
- [13] Silvain J-F, Veillere A, Heintz J-M, Vincent C, Guillemet T, Lacombe G, Lu Y, Chandra N (2012) The role of controlled interfaces in the thermal management of copper–carbon composites. *Emerg Mater Res* 1:75–88
- [14] Edtmaier C, Bauer E, Weber L, Tako ZS, Segl J, Friedbacher G (2015) Temperature dependence of the thermal boundary conductance in Ag–3Si/diamond composites. *Diam Relat Mater* 57:37–42
- [15] Monachon C, Schusteritsch G, Kaxiras E, Weber L (2014) Qualitative link between work of adhesion and thermal conductance of metal/diamond interfaces. *J Appl Phys* 115:123509
- [16] Anke K, Daniel L (2012) Functionality is key: recent progress in the surface modification of nanodiamond. *Adv Funct Mater* 22:890–906
- [17] Edtmaier C, Bauer E, Segl J, Foelske-Schmitz A, Pambaguian L (2016) Thermophysical behavior of diamond composites for diode laser heat sink applications at temperatures between 4 K and ambient. In: 46th international

- conference on environmental systems, Texas Tech University Library, Vienna, 2016, pp 1–14
- [18] Monje IE, Louis E, Molina JM (2013) Optimizing thermal conductivity in gas-pressure infiltrated aluminum/diamond composites by precise processing control. *Compos A Appl Sci Manuf* 48:9–14
- [19] Monje IE, Louis E, Molina JM (2012) Aluminum/diamond composites: a preparative method to characterize reactivity and selectivity at the interface. *Scr Mater* 66:789–792
- [20] Bruggeman DAG (1935) Berechnung verschiedener physikalischer Konstanten von heterogenen Substanzen. I. Dielektrizitätskonstanten und Leitfähigkeiten der Mischkörper aus isotropen Substanzen. *Ann Phys* 416:665–679
- [21] Hasselman DPH, Johnson LF (1987) Effective thermal conductivity of composites with interfacial thermal barrier resistance. *J Compos Mater* 21:508–515
- [22] Yamamoto Y, Imai T, Tanabe K, Tsuno T, Kumazawa Y, Fujimori N (1997) The measurement of thermal properties of diamond. *Diam Relat Mater* 6:1057–1061
- [23] Warmuzek M (2004) Aluminum-silicon casting alloys: atlas of microfractographs. ASM International, Materials Park
- [24] Tan Z, Li Z, Xiong D-B, Fan G, Ji G, Zhang D (2014) A predictive model for interfacial thermal conductance in surface metallized diamond aluminum matrix composites. *Mater Des* 55:257–262
- [25] Monachon C, Weber L (2015) Influence of a nanometric Al<sub>2</sub>O<sub>3</sub> interlayer on the thermal conductance of an Al/(Si, diamond) interface. *Adv Eng Mater* 17:68–75
- [26] Qi Y, Hector LG (2003) Hydrogen effect on adhesion and adhesive transfer at aluminum/diamond interfaces. *Phys Rev B* 68:201403
- [27] Qi Y, Hector LG (2004) Adhesion and adhesive transfer at aluminum/diamond interfaces: a first-principles study. *Phys Rev B* 69:235401
- [28] Wang X-G, Smith JR (2001) Copper/diamond adhesion and hydrogen termination. *Phys Rev Lett* 87:186103
- [29] Cheng DH, Xu WY, Zhang ZY, Yiao ZH (1997) Electroless copper plating using hypophosphite as reducing agent. *Met Finish* 95:34–37
- [30] Beffort O, Khalid FA, Weber L, Ruch P, Klotz UE, Meier S, Kleiner S (2006) Interface formation in infiltrated Al(Si)/diamond composites. *Diam Relat Mater* 15:1250–1260